Influence of antiferromagnetic ordering on the band structure of La_2CuO_4

S. G. Ovchinnikov

L. V. Kirenskiĭ Institute of Physics, Russian Academy of Sciences, Siberian Branch, 660036 Krasnoyarsk, Russia

(Submitted 26 April 1994; resubmitted 20 October 1994)
Zh. Éksp. Teor. Fiz. **107**, 796–811 (March 1995)

The band structure of the antiferromagnetic phase of La_2CuO_4 has been calculated in the generalized tight-binding approximation with consideration of the strong electron correlations in the CuO_2 layers. It has been shown that the magnetic moment of the sublattice forms as a result of redistribution of the partial spin-up and spin-down densities of states without splitting into energy sublevels. The quasiparticle dispersion law near the bottom of the conduction band is consistent with the result obtained in the $t-J$ model. The changes in the photoemission and inverse photoemission spectra upon the transition from the paramagnetic phase to the antiferromagnetic phase have been predicted. The available experimental data on photoemission from the La_2CuO_4 valence band are in qualitative agreement with our results. © *1995 American Institute of Physics.*

1. INTRODUCTION

There have been many attempts to eliminate the inconsistencies between the band-theory results which predict a metallic ground state for systems like La_2CuO_4, Nd_2CuO_4, and $YBa_2Cu_3O_6$ and the experimental data indicating the insulating character of the ground state of copper oxides.

In fact, according to the band-structure calculations in Refs. 1 and 2, a tight-binding $p-d$-hybridized band has a nested Fermi surface. Such a system is unstable toward the formation of a spin-density-wave (SDW) state, giving rise to a metal–insulator transition.[3,4] A similar mechanism for a metal–insulator transition operates in many oxides and sulfides of $3d$ metals.[5] However, the question of the electronic structure of copper oxides stemming from the SDW phase has not been resolved, since the undoped copper oxides just mentioned remain insulators as the temperature rises, although the SDW phase is destroyed above the Néel point and the system should pass into the metallic state.

The idea that the nature of the insulating state of La_2CuO_4 is specified by strong electron correlations has become widely accepted. Under conditions under which the energy U_d of the intersite correlations in copper is large compared with the charge-transfer energy $\delta=\varepsilon_p-\varepsilon_d$, i.e., $U_d>\delta$, the insulator gap E_g is determined by the charge-transfer energy.[6] Just such a mechanism for the formation of the insulator gap is postulated in the $p-d$ model of CuO_2 layers, which was proposed nearly simultaneously in Refs. 7 and 8. Subsequent band-structure calculations of La_2CuO_4 and Nd_2CuO_4 using the generalized tight-binding approximation, which explicitly includes the strong electron correlations, confirmed that the main contribution to the insulator gap in the paramagnetic phase is made by the charge-transfer energy.[9] Svane[10] arrived at the same conclusion as a result of a band-structure calculation of the antiferromagnetic phase of La_2CuO_4, using the density-functional formalism with consideration of the self-interaction.

The present work is devoted to a band-structure calculation of an undoped CuO_2 layer in the antiferromagnetic phase and its comparison with the structure in the paramagnetic phase. The hole dispersion laws and the density-of-states picture obviously change upon transition to the antiferromagnetic phase, but how much the insulator gap varies is unclear at the onset. The fact that antiferromagnetic ordering can make a contribution to the gap is clear from the foregoing discussion of spin-density waves. Spin-polaron narrowing of the conduction band, which causes a blue shift of the absorption edge, i.e., enlargement of the insulator gap upon transition to the antiferromagnetic phase, is also widely known for narrow-gap magnetic semiconductors.[11] As will be shown below, narrowing of the conduction band also occurs in our case, but the magnitude of the effect is strongly dependent on the state of the magnetic system. If it is assumed that the spins are classical, i.e., $\langle S^z\rangle=S=1/2$, hopping between neighboring cells is strictly forbidden and the narrowing of the band reaches a magnitude of the order of 100%. However, consideration of the zero-point quantum fluctuations leads to a half-width of the conduction band equal to $Z|t|\sqrt{n_0}$, where Z is the number of nearest neighbors, $|t|$ is the effective hopping integral, and $\tilde{n}_0$ is the concentration of magnons at $T=0$. As a result, the antiferromagnetic contribution to the insulator gap is suppressed, and in layered copper oxides, where the value of n_0 is small due to their quasi-two-dimensional nature, the shift of the band edge upon antiferromagnetic ordering amounts to a few percent.

The density-of-states picture near the gap edges varies more strongly. Upon the transition from the paramagnetic phase to the antiferromagnetic phase, the peak in the density of states at the bottom of the empty conduction band narrows and its intensity increases, while the peak near the top of the valence band weakens. These changes should be manifested in the photoemission and inverse photoemission spectra of La_2CuO_4 as the temperature is varied. Such changes in the photoemission spectra were, in fact, discovered by Takahashi *et al.*,[12] and our results are in qualitative agreement with the data in their paper.

 1063-7761/95/030451-09$10.00

2. MANY-ELECTRON MODEL OF COPPER OXIDES

It follows from the body of photoemission data that the bottom of the conduction band and the valence band at a depth of 6–7 eV are formed by the oxygen p orbitals and the copper d orbitals, while the remaining filled states are deeper and the empty states are higher. Therefore, we restrict ourselves to a calculation of the hybridized $p-d$ states of the CuO_2 layer, assuming that the effects of strong correlations are insignificant for the empty and filled bands and that these bands can be taken from standard band-structure calculations and simply superimposed on the $p-d$ band of the strongly correlated electrons.

We write the Hamiltonian of the p and d electrons of the CuO_2 layer in the hole representation:

$$H=H_d+H_p+H_{pd}+H_{pp}, \quad H_d=\sum_r H_d(r),$$

$$H_d(r)=\sum_{\lambda\sigma}\left[(\varepsilon_{d\lambda}-\mu)d^+_{r\lambda\sigma}d_{r\lambda\sigma}+\frac{1}{2}U_d n^{\sigma}_{r\lambda}n^{-\sigma}_{r\lambda}\right]$$

$$+\sum_{\sigma\sigma'}(V_d n^{\sigma}_{r1}n^{\sigma'}_{r2}-J_d d^+_{r1\sigma}d_{r1\sigma'}d^+_{r2\sigma'}d_{r2\sigma}),$$

$$H_p=\sum_i H(i),$$

$$H_p(i)=\sum_{\alpha\sigma}\left[(\varepsilon_{p\alpha}-\mu)p^+_{i\alpha\sigma}p_{i\alpha\sigma}+\frac{1}{2}U_p n^{\sigma}_{i\alpha}n^{-\sigma}_{i\alpha}\right]$$

$$+\sum_{\sigma\sigma'}(V_p n^{\sigma}_{i1}n^{\sigma'}_{i2}-J_p p^+_{i1\sigma}p_{i1\sigma'}p^+_{i2\sigma'}p_{i2\sigma}),$$

$$H_{pd}=\sum_{\langle i,r\rangle}H_{pd}(i,r),$$

$$H_{pd}(i,r)=\sum_{\alpha\lambda\sigma\sigma'}(T_{\lambda\alpha}p^+_{i\alpha\sigma}d_{r\lambda\sigma}+\text{H.c.}+V_{\lambda\sigma}n^{\sigma}_{r\lambda}n^{\sigma'}_{i\alpha}$$

$$-J_{\alpha\lambda}d^+_{r\lambda\sigma}d_{r\lambda\sigma'}p^+_{i\lambda\sigma'}p_{i\alpha\sigma}),$$

$$H_{pp}=\sum_{\langle i,j\rangle}\sum_{\alpha\beta\sigma}(t_{\alpha\beta}p^+_{i\alpha\sigma}p_{j\beta\sigma}+\text{H.c.}), \qquad (1)$$

where ε_p and ε_d are the one-particle energies of p and d holes, $U_p(U_d)$ and $V_p(V_d)$ are the matrix elements of on-site Coulomb repulsion in the same and different oxygen (copper) orbitals, $J_p(J_d)$ are the Hund exchange integrals, $T_{\lambda\sigma}$ and $t_{\alpha\beta}$ are the matrix elements for $p-d$ and $p-p$ hopping between nearest neighbors, $V_{\lambda\alpha}$ and $J_{\lambda\alpha}$ are the matrix elements of the Coulomb and exchange interactions of copper–oxygen nearest-neighbor pairs, μ is the chemical potential, σ and σ' are the projections of the hole spin, and $n_{r\lambda}(n_{i\alpha})$ is the number operator for holes in a copper (oxygen) ion. In (1) the first two terms describe the on-site energies with consideration of the Hubbard correlations U_d and U_p, the Coulomb interactions in different orbitals λ, and the Hund exchange. The last two terms in (1) describe the intersite $p-d$ hopping and interactions and the $p-p$ hopping. The significant orbitals are: $d_{x^2-y^2}$ ($\lambda=1$) and d_{z^2} ($\lambda=2$) for copper, p_x ($\alpha=1$) and p_y ($\alpha=2$) for oxygen. We introduce the notation

$$T_{x^2-y^2,p_x}=T_{pd}, \quad V_{x^2-y^2,p_x}=V_{pd},$$

$$J_{x^2-y^2,p_x}=J_{pd}, \quad t_{x,y}=t_{pp}.$$

Consideration of the crystal field results in splitting of the d and p hole levels:

$$\varepsilon_{z^2}=\varepsilon_d+\Delta_d, \quad \varepsilon_d\equiv\varepsilon_{x^2-y^2}, \quad \varepsilon_{py}=\varepsilon_p+\Delta_p, \quad \varepsilon_p\equiv\varepsilon_{px}.$$

From the general properties of d orbitals we have

$$T_{z^2,p_x}=T_{pd}/\sqrt{3}.$$

3. BRIEF DESCRIPTION OF THE GENERALIZED TIGHT-BINDING APPROXIMATION

The idea of calculating the band structure with exact calculation of the strong electron correlations was described in Ref. 13, and details of the calculation of dispersion laws and the one-particle density of states in the paramagnetic phase were given in Refs. 14 and 15, respectively. The essence of the method is a combination of accurate diagonalization of the many-electron Hamiltonian for small clusters followed by approximate description of the intercluster hopping and Coulomb interactions.

The lattice of the CuO_2 layer is divided into two sublattices, whose points are CuO_2 clusters. The calculations are conveniently performed in the hole representation, and the $p^6d^{10}p^6$ configuration with a number of holes $n_h=0$ is then the vacuum state $|0\rangle$. The eigenstates of a cluster are characterized by the number of holes n, the spin, the projection of the spin, and the orbital quantum numbers. For example, for $n=1$ the eigenstates are mixtures of the $p^5d^{10}p^6$ and $p^6d^9p^6$ configurations, and for $n=2$ they are mixtures of the $p^5d^{10}p^5$, $p^5d^9p^6$, $p^6d^8p^6$, and $p^4d^{10}p^6$ configurations. Actual calculations were performed in a six-band model, in which two orbitals were taken into account in each ion: $d_{x^2-y^2}$ and d_{z^2} in the copper ion and p_x and p_y in each oxygen ion. The states of the apical oxygen ions, which lie outside of the CuO_2 layer, are always occupied and determine the strength of the crystal field, i.e, renormalize the value of the parameter $\delta=\varepsilon_p-\varepsilon_d$. We assumed that such renormalization has already been performed, and we shall not explicitly take into account the apical oxygen atoms.

An essentially similar method for calculating the electronic structure of the CuO_2 layer was used in Ref. 16, where a simpler three-band $p-d$ model was considered and exact diagonalization was performed for a CuO_4 cluster. At first glance, our use of the division of the lattice into CuO_2 clusters violates the square symmetry, but this is not so. The unit cell in our division consists of two CuO_2 clusters, i.e., a vertical cluster and a horizontal cluster (see Refs. 13–15) and has the required square symmetry despite the fact that an individual linear CuO_2 cluster does violate the symmetry. The situation is completely analogous to two magnetic sublattices in a Heisenberg antiferromagnet. In addition, such division is especially convenient for calculations of the antiferromagnetic phase. We note that after accurate diagonaliza-

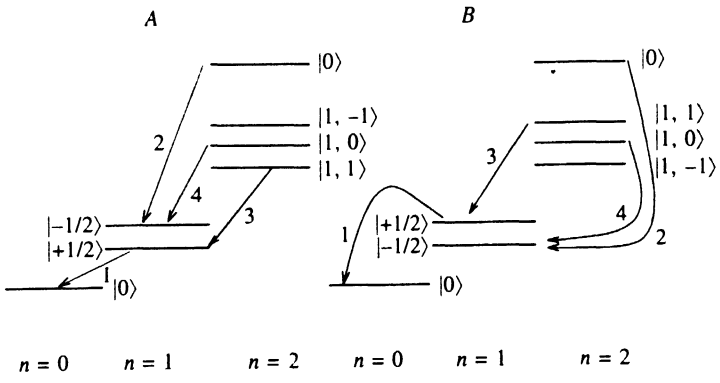

FIG. 1. Diagram of the lower levels of the multiplets with $n=0$, 1, and 2 for sublattices A and B. The lines with an arrow show transitions with annihilation of a spin-up hole, and the numbers near them label these transitions. For the sake of simplicity, the excited levels for $n=1$ and $n=2$ are not shown.

tion of the cluster Hamiltonian, the expression for the complete Hamiltonian in the form of the sum of interacting clusters is exact, and all subsequent approximations relate only to the method for taking into account the intercluster hopping and interactions.

The many-electron approach with a finite number of cluster states unavoidably leads to the algebra of Hubbard operators, if we wish to maintain the exact commutation relations for the Fermi and spin operators, as well as the local restrictions on the filling of the many-electron terms due to strong correlations. One-particle Fermi excitations in a cluster are transitions from an n-particle state to an $(n+1)$-particle state and have the energy

$$\Omega_\sigma(m)=E(n+1,l1)-E(n,l2),$$

where σ is the projection of the spin, m labels different transitions of the type $|n\rangle\rightarrow|n+1\rangle$, and $l1$ and $l2$ are the allowed orbital states of the many-electron terms.

Intercluster hopping results in the formation of the bands $\Omega_\sigma(m,k)$. Due to the correlation effects the effective hopping integral $\tilde{t}\ll t$.[13] Moreover, $\tilde{t}\ll E_g$, whence it is clear that undoped CuO_2 layers are far from the Mott insulator–metal transition. In this case the inclusion of intercluster hopping can be described in the "Hubbard I" approximation (which is equivalent to the Hartree–Fock approximation in the diagram technique for Hubbard operators[17]), whose corrections contain the small parameter $\tilde{t}/E_g$ and can be calculated using the diagram technique for Hubbard operators (X).

We note that the bands appearing under our approach are bands of quasiparticles, whose statistics do not coincide in the general case with Fermi statistics or with Bose statistics and are determined by complex commutation relations for Hubbard operators. The number of states in each band can be fractional and depends on the concentration of electrons. In particular, with consideration of the spin, each band for an undoped CuO_2 layer with a number of holes per molecule $n_h=1$ contains only one state, rather than the two states observed for free electrons. This property is often ascribed to spinless fermions (holons), although the situation is more complicated, since spin degeneration is conserved in our approach in both the paramagnetic and antiferromagnetic phases.

4. SPECIAL FEATURES OF THE CALCULATION FOR THE ANTIFERROMAGNETIC PHASE

In higher-order perturbation theory with respect to $\tilde{t}/E_g$ in the undoped case, in which the number of holes in the system coincides with the number of CuO_2 clusters, hopping is known to result in an effective Heisenberg Hamiltonian with antiferromagnetic exchange J_0. In principle, J_0 can be calculated on the basis of calculations of the band structure in the paramagnetic phase, but due to the large number of participating virtual processes this calculation is a problem in its own right, which is beyond the scope of the present work.

We assume that J_0 is known: $J_0\sim 0.1$ eV.[18] In the antiferromagnetic phase the molecular exchange field $h_i=J_0\langle S_i^z\rangle$ splits the local levels $\Omega_\sigma(i,m)$:

$$\Omega_\sigma(i,m)=\Omega_\sigma(m)-\sigma h_i,\quad \sigma=+1/2,-1/2. \tag{2}$$

Here the subscript i labels sublattices 1 and 2, $\langle S_1^z\rangle\equiv\langle S^z\rangle$, and $\langle S_2^z\rangle=-\langle S^z\rangle$. The method developed in Refs. 13–15 to calculate the band structure and density of states of Fermi quasiparticles is easily generalized to the case of the antiferromagnetic phase. Let X_k^m and Y_k^m be the Fourier transforms of the Hubbard operators in sublattices 1 and 2. We define the two-sublattice Green's function

$$\hat{D}^\sigma_{mn}(\mathbf{k},E)=\begin{pmatrix}\langle\langle X^m_{\mathbf{k},\sigma}|X^{+n}_{\mathbf{k},\sigma}\rangle\rangle, & \langle\langle X^m_{\mathbf{k},\sigma}|Y^{+n}_{\mathbf{k},\sigma}\rangle\rangle\\ \langle\langle Y^m_{\mathbf{k},\sigma}|X^{+n}_{\mathbf{k},\sigma}\rangle\rangle, & \langle\langle Y^m_{\mathbf{k},\sigma}|Y^{+n}_{\mathbf{k},\sigma}\rangle\rangle\end{pmatrix}. \tag{3}$$

The zeroth (intracluster) Green's functions equal

$$D^{ij,\sigma}_{0,mn}(\mathbf{k},E)=\delta_{ij}\delta_{mn}\frac{F_\sigma(i,m)}{E-\Omega_\sigma(i,m)},$$

where $F_\sigma(i,m)$ are end factors,[17] which equal

$$F_\sigma(i,m)=\langle\{X^m_{i,\sigma},X^{+m}_{i,\sigma}\}_+\rangle. \tag{4}$$

In the Hartree–Fock approximation with respect to hopping, the inverse Green's function (3) equals

$$\hat{D}^{-1}=\hat{D}_0^{-1}-\hat{A}-\hat{B}, \tag{5}$$

where the matrices $\hat{A}$ and $\hat{B}$ describe $p-d$ and $p-p$ hopping. Their explicit forms were presented in Refs. 14 and 15 and are not reproduced here in view of their cumbersomeness. The main details of the motion of a hole on the background of an antiferromagnetic matrix are associated with the varia-

TABLE I. Occupation numbers of lower cluster levels.

State		Sublattice A	Sublattice B
$n=1$	$\|+1/2\rangle$	$(1-x)(1-a_1)$	$(1-x)a_1$
	$\|-1/2\rangle$	$(1-x)a_1$	$(1-x)(1-a_1)$
$n=2$	$\|1,+1\rangle$	$x(1-a_2)$	xa_2^2
	$\|1,0\rangle$	$xa_2(1-a_2)$	$xa_2(1-a_2)$
	$\|1,-1\rangle$	xa_2^2	$x(1-a_2)$

tion of the local occupation numbers of the one- and two-hole terms, through which the end factors are expressed, rather than with the exchange splitting (2). Figure 1 shows the lower sublevels for each of the subspaces of the Hilbert space with a different number of holes per cluster $n=0$, 1, and 2. The lines with an arrow depict various Fermi transitions with annihilation of a hole with spin up. The total number of such transitions having nonzero end factors for each sublattice in our problem equals 28.

The end factors, which, according to (4), are equal to the sum of the occupation numbers of the initial and final states, are found self-consistently together with the solution of the equation for the chemical potential

$$\sum_{n,l} n\langle X^{n,l;n,l}\rangle = n_h \tag{6}$$

and for the magnetic moment of the sublattice $\langle S_i^z\rangle$. Here n_h is the number of holes per formula unit, which equals $n_h=1+x$ for systems of the $La_{2-x}Sr_xCuO_4$ type. According to (6), the ground one-particle term for p-type systems is filled with a probability $1-x$, and the two-particle state is filled with a probability x. We find $\langle S^z\rangle$ within each subspace with a fixed occupation number from the solution of the Heisenberg model: with $S=1/2$ for $n=1$ and $S=1$ for $n=2$. Here it is convenient to utilize the formulation of the Heisenberg model in the Hubbard-operator representation,[19] which makes it possible to find at once the occupation numbers of the different spin sublevels along with $\langle S^z\rangle$. The results of the calculations are presented in Table I, where a_1 and a_2 are the temperature-dependent concentrations of magnons for $S=1/2$ and $S=1$, respectively:

$$S=1/2, \quad \langle S^z\rangle = 1/2 - a_i,$$

$$S=1, \quad \langle S^z\rangle = 1 - a_2 - a_2^2. \tag{7}$$

5. BAND STRUCTURE IN THE ANTIFERROMAGNETIC PHASE

The results of the solution of the dispersion equation

$$\det\|\hat{D}_0^{-1} - \hat{A} - \hat{B}\| = 0 \tag{8}$$

are presented in Figs. 2–4 for the undoped case, $x=0$. The set of model parameters corresponding to La_2CuO_4 from Ref. 9 was used:

$$U_d = U_p = \infty, \quad V_d = 4.5, \quad V_p = 3, \quad V_{pd} = 0.6,$$

$$J_d = J_p = 0.5, \quad J_{pd} = 0.2, \quad T_{pd} = 1,$$

$$t_{pp} = 0.2, \quad \delta = 2, \quad \Delta_d = 1.5, \quad \Delta_p = 0.8.$$

The energy is taken in the hole representation; therefore, the valence band lies above the conduction band. The level from which the hole energy is measured is $\varepsilon_d=0$. The density of states for the paramagnetic phase of La_2CuO_4 was calculated with the same set of parameters as in Ref. 15. We note that the hole spectrum is spin-degenerate. The lower Hubbard bands $\Omega_\sigma^{\pm}(1,\mathbf{k})$ (there are two of them due to the two-sublattice structure) with $m=1$ form mainly as a result of $|0\rangle \to |1,\sigma\rangle$ transitions. If only the intraband hopping is left in matrices $\hat{A}$ and $\hat{B}$, it is easy to obtain the analytic expression

$$\Omega_\sigma^{\pm}(1,\mathbf{k}) = \Omega(1) \pm \sqrt{J_0^2\langle S^z\rangle^2 + T_1^2\gamma^2(\mathbf{k})F_\sigma(1,1)F_\sigma(2,1)}. \tag{9}$$

Here $T_1 = T_{pd}uv/\sqrt{2} = 2T_{pd}^2/\nu$, and

$$\gamma(\mathbf{k}) = 2(\cos k_x a + \cos k_y a),$$

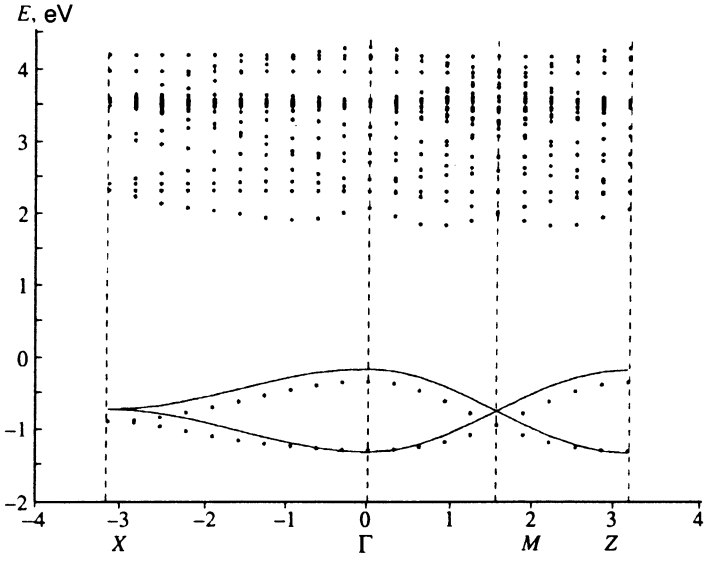

FIG. 2. Hole band structure in the paramagnetic state of an undoped CuO_2 layer. The solid lines are described by Eq. (11).

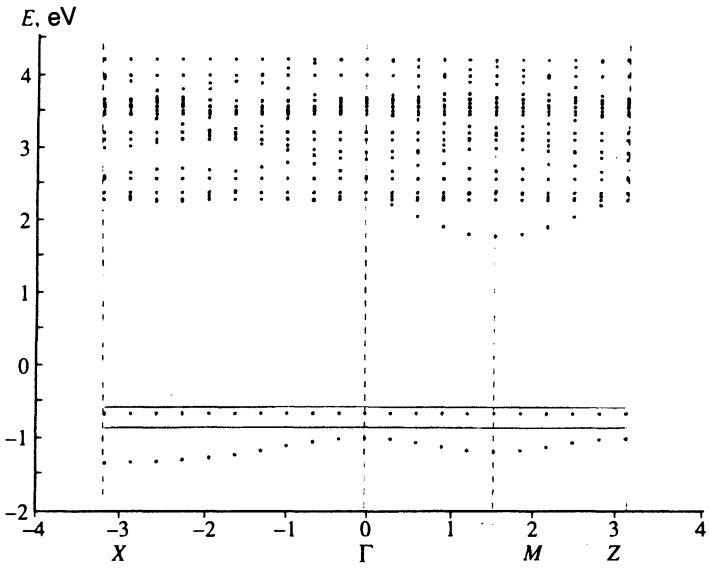

FIG. 3. Hole band structure in the antiferromagnetic state of an undoped CuO_2 layer with $\langle S^z\rangle=1/2$.

where a is the lattice constant and the coefficients u and v define the wave function of the $n=1$ ground state term

$$|1,\sigma\rangle=u|0,d_{x^2-y^2}\sigma,0\rangle-v(|p_x\sigma,0,0\rangle + |0,0,p_x\sigma\rangle)/\sqrt{2},$$

and are given by the expressions

$$u^2=\frac{1}{2}\left(1+\frac{\delta}{\nu}\right), \quad v^2=1-u^2, \quad \nu^2=\delta^2+8T_{pd}^2.$$

The product of the occupation numbers in the different sublattices,

$$F_\sigma(1,1)F_\sigma(2,1)=(\tfrac{1}{2}+2\sigma\langle S^z\rangle)(\tfrac{1}{2}-2\sigma\langle S^z\rangle)=\tfrac{1}{4}-\langle S^z\rangle^2, \tag{10}$$

does not depend on the projection of the spin and is determined by the concentration of magnons. As a result, for the spectrum of the lower Hubbard band we obtain

$$\Omega_\sigma^{\pm}(1,\mathbf{k})=\Omega(1) \pm\sqrt{J_0^2\left(\frac{1}{2}-a_1\right)^2+T_1^2\gamma^2(\mathbf{k})a_1(1-a_1)}. \tag{11}$$

This spectrum is depicted by the solid lines in Figs. 2–4. It is seen that the contribution of interband transitions is, in fact, small and basically reduces to a small constant shift.

The number of states in each Hubbard band is determined by the end factor, and in the paramagnetic phase for the bands (11) we have $F(1)=1/2$. In the antiferromagnetic phase it depends on the magnetization, but the sum equals

$$F_\sigma(1,1)+F_\sigma(2,1)=1.$$

With consideration of the spin, the total number of states in the bands (11) equals two, which equals the number of holes

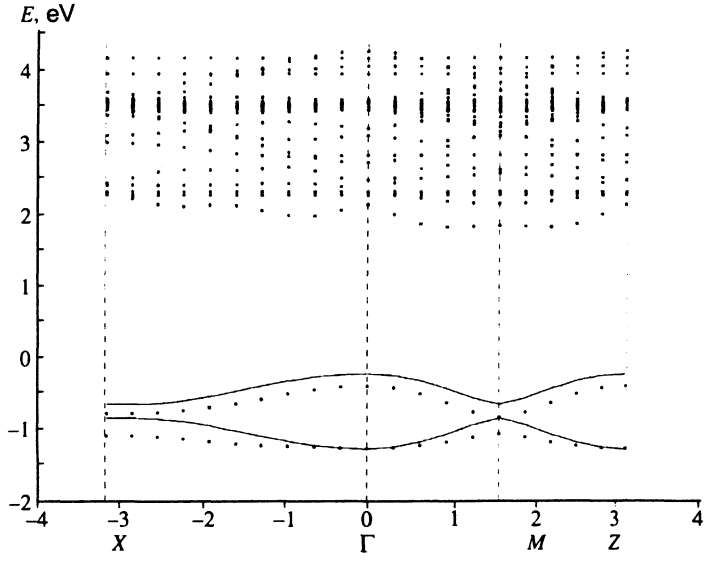

FIG. 4. Hole band structure in the antiferromagnetic state of an undoped CuO_2 layer with $\langle S^z\rangle=0.22$.

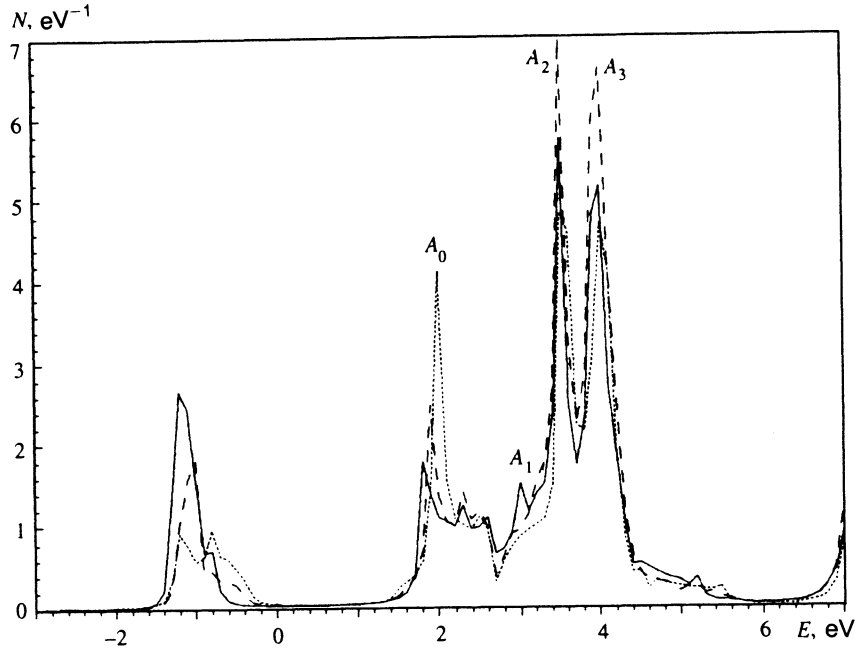

FIG. 5. Hole density of states in an undoped CuO_2 layer. The dashed line corresponds to the paramagnetic phase, the solid line corresponds to the antiferromagnetic phase with $\langle S^z\rangle=1/2$, and the dotted line corresponds the antiferromagnetic phase with $\langle S^z\rangle=0.22$.

in the unit cell containing two CuO_2 clusters when $x=0$. Thus, the lower bands $\Omega_\sigma^{\pm}(1,\mathbf{k})$ are completely filled, since these bands correspond to empty bands in the electronic representation, and the Fermi level lies in the insulator gap.

We consider two possible descriptions of the antiferromagnetic phase: in the mean-field approximation, where $\langle S^z\rangle=1/2$ (Fig. 3), and with consideration of the zero-point quantum fluctuations (Fig. 4). The value $\langle S^z\rangle=0.22$ in the latter case was previously obtained in Ref. 14 using the spin-wave theory of a quasi-two-dimensional Heisenberg antiferromagnet with a ratio of interplanar exchange to intraplanar exchange $J_1/J_0=10^{-5}$, which corresponds to layered copper oxides.[18] A similar value $\langle S^z\rangle\approx 0.3$ was obtained for a two-dimensional Heisenberg antiferromagnet with $S=1/2$ using linear spin-wave theory in Ref. 20, where a comparison with the results of exact numerical calculations was made and it was shown that the corrections to the results of linear spin-wave theory are small.

In our approach the calculation of the hole density of states is more tedious than the calculation of the spectrum, since it requires knowledge of the entire Green's function in (3), rather than only its pole. This problem was solved for the paramagnetic phase in Ref. 16, and generalization to the antiferromagnetic phase requires, as in the case of the spectrum, consideration of the variation of the occupation numbers due to the exchange splitting of the levels $\Omega_\sigma(i,m)$ (2). The final expression for the hole density of states has the form

$$N(E)=\frac{2}{N}\sum_{\mathbf{k}\sigma}\sum_{\lambda m}|\gamma_\lambda(m)|^2\left(-\frac{1}{\pi}\right)Jm[D_{mm}^{11,\sigma}(\mathbf{k},E+i\varepsilon)+D_{mm}^{22,\sigma}(\mathbf{k},E+i\varepsilon)], \tag{12}$$

where $\gamma_1(m)$ are the Clebsch–Gordan coefficients, which give a representation of the one-electron operator $a_{f\lambda\sigma}$ in terms of the Hubbard operators $X_{f,\sigma}^m$ (see Refs. 14 and 15). The density of states is presented in Fig. 5 for different values of the magnetic moment of the sublattice.

6. CALCULATION OF THE MAGNETIZATION OF A SUBLATTICE

In the antiferromagnetic phase the band structure and the density of states are spin-degenerate. However, the sublattice density of states can be determined for a given spin:

$$N_{A,\sigma}(E)=\frac{2}{N}\sum_{\mathbf{k}}\sum_{\lambda m}|\gamma_\lambda(m)|^2\left(-\frac{1}{\pi}\right)JmD_{mm}^{11,\sigma}(\mathbf{k},E+i\varepsilon), \tag{13}$$

which depends on the projection of the spin. Clearly, $N_{B,-\sigma}(E)=N_{A,\sigma}(E)$. The partial spin densities of states $N_+=N_{A,+}+N_{B,-}$ and $N_-=N_{A,-}+N_{B,+}$ are shown in Fig. 6 for three values of $\langle S^z\rangle$, which are equal to 0.5, 0.22, and 0.10, respectively. We note that in the Hubbard model the density of states N_- for the lower Hubbard band would be equal to zero when $\langle S^z\rangle=0.5$. In our case $N_-\neq 0$, although it is small. This is attributed to the weak covalent mixing of the oxygen p states with the lower Hubbard band, which reduces the magnetic moment at the copper atom in comparison with the nominal value in the Heisenberg model by about 15%.[14] We stress that in the many-electron approach developed here, the formation of the magnetic moment is due to redistribution of the occupation numbers of the spin sublevels, rather then to the large splitting of the spin subbands obtained in the one-electron approach.

The difference between the spin densities of states for the valence band is more complicated: both variation of N_+ and N_- and splitting of the maxima of N_+ and N_- occur near the top of the band. The narrow peak in the deeper part of the valence band with $E=3.5$ eV, which redistributes its intensity most strongly upon antiferromagnetic ordering, is associated with the copper d_{z^2} states. Consideration of the

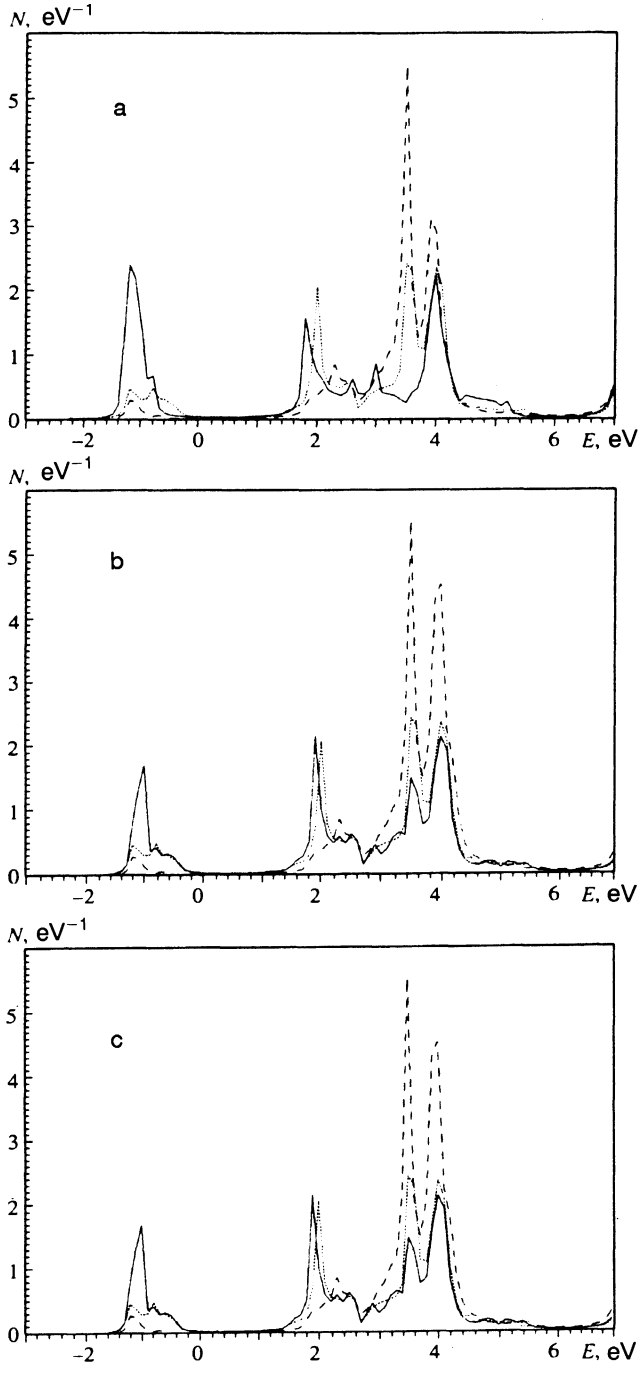

FIG. 6. Intralattice density of states for $\langle S^z\rangle=0.5$ (a), 0.22 (b), and 0.1 (c). Solid line—spin up, dotted line—spin down, dashed line—paramagnetic phase.

quantum fluctuations (Fig. 6b) preserves the picture just described as a whole, causing only quantitative changes.

We have hitherto calculated $\langle S^z\rangle$ self-consistently in the Heisenberg model. Knowing the spin density of states, we can calculate

$$\langle S^z\rangle=\frac{1}{2}\int_{-\infty}^{\varepsilon_F}[N_+(E)-N_-(E)]dE, \tag{14}$$

which gives 0.42, 0.26, and 0.12, respectively, for cases a, b, and c in Fig. 6. The agreement between the results of the band and localized approaches is adequate.

The density of states in Fig. 6c illustrates the influence of the temperature dependence of the magnetization of the sublattice on the band structure. As is clear from Fig. 1, as the excited terms are filled with increasing temperature, the spin sublevels of each multiplet are primarily populated, i.e. $\langle S^z\rangle$ varies. The remaining temperature corrections play a far lesser role, since they are exponentially small.

A similar picture of the formation of the magnetic moment in antiferromagnetic oxides of $3d$ metals was obtained in Ref. 21. At the same time, calculations using the density-functional formalism, even with consideration of corrections for the self-interaction, which ensure an insulating ground state, give a gap and a magnetic moment due to the large splitting of the spin subbands.[10] Conclusions regarding the formation of a magnetic moment due to redistribution of spin densities of states without significant splitting into energy sublevels were previously drawn in the many-electron theory of magnetic semiconductors for chromium chalcogenide spinels[22] and europium monochalcogenides.[23]

7. COMPARISON WITH DATA FROM PHOTOELECTRON SPECTROSCOPY

As is seen from Fig. 5, the density of states of the valence band varies differently upon the transition from the paramagnetic phase to the antiferromagnetic phase, depending on the energy. Peak A_0 near the top of the band with $E_0=2$ eV weakens and shifts slightly toward smaller energies, while peak A_1 with $E=3$ eV, peak A_2 with $E_2=3.6$ eV, and peak A_3 with $E_3=4.2$ eV increase in intensity.

These conclusions may be compared with the photoemission spectra of La_2CuO_4 measured at $T=300$ K and $T=150$ K.[12] Peak A_0 did not appear in the spectrum, apparently due to the small value of the matrix element of the dipole transition near the top of the band. Peaks A_1, A_2, and A_3 may be correlated with peak A_1 with a width of $\sim$1 eV in Ref. 12, whose intensity decreased with increasing temperature. Such behavior is consistent with our results. The higher-energy peaks with binding energies of 5 eV or more cannot be discussed in our model, since the copper t_{2g} states,[2] which are not taken into account in the present calculation using a six-band model, lie 4 eV below the top of the valence band.

According to our calculations, the density of states peak near the bottom of the conduction band decreases in intensity and broadens as the temperature decreases. The same variations should be observed in the inverse photoemission spectra. Unfortunately, we do not know of any data on the temperature dependence of these spectra for undoped La_2CuO_4.

8. DISCUSSION OF THE RESULTS OF THE BAND-STRUCTURE CALCULATIONS

The problem of the motion of a hole on the background of an antiferromagnetic lattice is a spin polaron problem, and this problem has been solved for CuO_2 layers by many investigators in simpler models.[24–27] At first glance, it follows from Eq. (2) that we describe the interaction of a carrier with

a spin lattice in the mean-field approximation and ignore the spin-polaron effects. This would also be the case for ordinary bands of free electrons, for which the numerator of the Green's function is always equal to unity. In our case the variation of the end factors (the residues of the Green's function) induced by the splitting (2), rather than the splitting itself, has the main influence on the electronic structure. These factors are calculated using exact diagonalization of the cluster, as a result of which all local spin-flip processes are taken into account. A similar calculation for the narrow-band $s-d$ model with exact consideration of the local exchange of the carrier and the lattice spin[28] demonstrated correspondence with the results of the traditional variational description of a spin polaron[11] in an antiferromagnetic semiconductor.

Let us compare the band structure in the paramagnetic and antiferromagnetic phases. The dispersion law of the valence band, which consists of a large number of narrow hole upper Hubbard bands, changes near the band edge. Redistribution of the intensities of the narrow density-of-states peaks occurs in the depth of the valence band. The conduction band undergoes greater changes. In the mean-field approximation for the magnetization, the lower Hubbard bands narrow drastically (see Fig. 3), and a large shift ΔE of the bottom of the conduction band appears as a consequence. The antiferromagnetic contribution to the insulator gap equals $\Delta E \approx 0.5$ eV. At the same time, consideration of the zero-point quantum fluctuations largely restores the dispersion of the states near the bottom of the conduction band and the top of the valence band, approximating it to that for the paramagnetic phase (compare Fig. 2 and Fig. 4). The densities of states continue to differ in intensity, since the end factors for the two lowest Hubbard bands differ from one another and from the paramagnetic value.

As is seen from Fig. 5, consideration of the spin fluctuations almost completely suppresses the antiferromagnetic contribution ΔE to the insulator gap. The reason for the suppression of the spin-polaron narrowing becomes clear from an analysis of Eq. (11). The band edge in the paramagnetic phase is

$$\Omega^{+}_{PM}=\Omega(1)+2T_1.$$

In the antiferromagnetic phase the edge of the same band is

$$\Omega^{+}_{AFM}=\Omega(1)+\sqrt{\frac{J_0^2}{4}+(16T_1^2-J_0^2)a_1(1-a_1)}.$$

In the absence of spin fluctuations, a large shift of the band edge $\Delta E=2T_1-J_0/2$ is obtained, since for La_2CuO_4 we have $2T_1\approx 0.4$ eV (Ref. 15) and $J_0=0.1$ eV. According to Eqs. (9)–(11), the effective hopping integral is

$$T_{\text{eff}}=T_1\sqrt{F_\sigma(1,1)F_\sigma(2,1)}=T_1\sqrt{\frac{1}{4}-\langle S^z\rangle^2}. \qquad (15)$$

In the paramagnetic phase, where the fluctuations are maximal, $T_{\text{eff}}=0.5T_1$. In the antiferromagnetic phase $T_{\text{eff}}=T_1\sqrt{a_1(1-a_1)}$, which amounts to $0.45T_1$ when $a_1=0.28$. The square-root dependence on the magnon concentration increases their contribution to the energy of the bottom of the conduction band and results in compensation of the spin-polaron narrowing of the band. This effect is appreciable even for cubic isotropic antiferromagnets with a small concentration of zero-point magnons. For example, for $a_1=0.1$ we obtain $\sqrt{a_1(1-a_1)}=0.3$, so that even such a small concentration of zero-point magnons compensated 60% of the decrease in the effective hopping integral. Nevertheless, a phenomenon involving displacement of the band edge and associated displacement of the absorption edge is known in antiferromagnetic semiconductors.[11] As follows from our work, there should be no displacement of the absorption band for La_2CuO_4 due to the large contribution of the zero-point fluctuations.

A conclusion that hole hopping is caused by spin fluctuations was previously drawn in the context of the $t-J$ model.[29] This circumstance distinguishes a spin polaron in a system with strong electron correlations from an ordinary polaron and a spin polaron in systems with weak correlations, where there is a priming kinetic energy in the absence of phonons or magnons.

To understand the degree of applicability of our calculations in the Hubbard I approximation to intercluster hopping, we compare the results with data from the exact diagonalization of small clusters using the Lanczos algorithm for the Hubbard model,[30] the $t-J$ model,[29] and the three-band $p-d$ model.[31] The quasiparticle dispersion law was discussed in all of these studies. A comparison of perturbation theory for $J<t$ with the exact results in the $t-J$ model reveals that the corrections to the peaks are small.[29] Similarly, it was shown in the Hubbard model in the undoped case that the spectral density can be described in the mean-field (spin-density-wave) theory with self-consistent calculation of the magnetization of the sublattice in spin-wave theory.

The expression obtained for the dispersion law of a spin polaron in the $t-J$ model is[26,27,32–35]

$$E(\mathbf{k})=\frac{J}{2}(\cos k_x a+\cos k_y a)^2+\varepsilon_0$$
$$=t_2\cos k_x a\cos k_y a+t_3(\cos 2k_x a+\cos 2k_y a)+\tilde{\varepsilon}_0, \qquad (16)$$

which corresponds to the hopping of a free particle between second and third nearest neighbors in the tight-binding approximation. It follows from our Eq. (11) that although the region of $\mathbf{k}$ space where $\gamma(\mathbf{k})$ is small is close to the Fermi surface of free electrons in the tight-binding approximation, the expansion of (11) in the small parameter $T_{\text{eff}}\gamma(\mathbf{k})/J_0\langle S^z\rangle$ in this region gives the quasiparticle dispersion law

$$\Omega^{\pm}(\mathbf{k})=\Omega_1^{\pm}J_0\langle S^z\rangle^{\pm}T_1^2a_1(1-a_1)\gamma^2(k)/J_0\langle S^z\rangle, \qquad (17)$$

which coincides with (16) with respect to the character of the dispersion. At the same time, dispersion of the type $\sqrt{\gamma^2(\mathbf{k}+\text{const})}$ is obtained far from the Fermi surface of free electrons both in our case and in the Hubbard model.[30] As is seen from Fig. 4, the bottom of the hole upper Hubbard band (the top of the electron valence band) is located near the point $(\pi/2,\pi/2)$ of the Brillouin zone on the ΓM [1,1] axis, in accordance with the results in Ref. 36.

Thus, a comparison of our approximate results and the results from Refs. 29 and 30 with the data from accurate numerical diagonalization of small clusters[29,31] reveals that if the mean-field theory takes into account the quantum spin fluctuations, the higher corrections to it are insignificant. The physical reason for this, as was noted above, is that the La_2CuO_4 system is far from the Mott–Hubbard transition point and there is a small parameter T_{eff}/E_g. A similar conclusion was previously drawn in Ref. 37.

9. CONCLUSIONS

A more exact theory should employ a nonlinear theory of spin waves in a quasi-two-dimensional antiferromagnet, rather than a linearized approach. However, we are confident that such a refinement will result only in quantitative changes. In fact, the concentration of zero-point magnons will vary, but will still be of the same order. The qualitative aspect of the influence of zero-point magnons on the displacement of the band edge defined by Eq. (15) does not depend on the concentration of magnons.

The next remark refers to the role of doping by holes. The principal change in the density of states upon doping is associated with the appearance of in-gap states, but this effect is not associated with antiferromagnetic ordering and will, therefore, not be discussed here. We shall likewise not discuss the suppression of antiferromagnetism upon doping by electrons or holes. This question was considered using accurate diagonalization of the Hamiltonian of Emery's model in Ref. 38.

As for the spin-polaron narrowing of the band, the table of occupation numbers reveals that when $x \neq 0$,

$$T_{\text{eff}} \sim T_1 \sqrt{x + a_1}.$$

The dependence $T_{\text{eff}} \sim T\sqrt{x}$ was previously obtained in the narrow-band $s-d$ model[28] and in the $t-J$ model[39] when the zero-point quantum fluctuations were disregarded. Since the minimal value for a cubic isotropic antiferromagnet is $a_1 = 0.0675$,[40] the contribution of the carriers to the width of the band is small when $x < 0.01$.

In conclusion we note that the generalized tight-binding approximation developed here permits calculation of the band structure of copper oxides with explicit consideration of the strong electron correlations in both the paramagnetic and antiferromagnetic phases. The dispersion law of the quasiparticles (spin polarons and holons) for the hole lower Hubbard band changes only slightly upon transition from the paramagnetic phase to the antiferromagnetic phase. At the same time, the heights of the peaks in the density of states and in the photoelectron spectra vary more strongly. Some of the temperature changes in the photoelectron spectra predicted in the present work are already known experimentally; others may be confirmed by photoemission and inverse photoemission investigations.

We thank the Scientific Council for High-T_c Superconductivity for financially supporting the present research as part of the "Hubbard" project under Grant No. 93237.

[1] L. F. Matheiss, Phys. Rev. Lett. **58**, 1028 (1987).
[2] W. E. Pickett, Rev. Mod. Phys. **61**, 433 (1989).
[3] L. V. Keldysh and Yu. V. Kopaev, Fiz. Tverd. Tela (Leningrad) **6**, 2791 (1964) [Sov. Phys. Solid State **6**, 2219 (1965)].
[4] A. N. Kozlov and L. A. Maksimov, Zh. Éksp. Teor. Fiz. **48**, 1184 (1965) [Sov. Phys. JETP **21**, 790 (1965)].
[5] R. O. Zaĭtsev, E. V. Kuz'min, and S. G. Ovchinnikov, Usp. Fiz. Nauk **148**, 603 (1986) [Sov. Phys. Usp. **29**, 322 (1986)].
[6] J. Zaanen, G. A. Sawatzky, and G. W. Allen, Phys. Rev. Lett. **55**, 418 (1985).
[7] V. J. Emery, Phys. Rev. Lett. **58**, 2794 (1987); C. M. Varma, S. Schmitt-Rink, and E. Abrahams, Solid State Commun. **62**, 681 (1987).
[8] Yu. B. Gaĭdideĭ and V. M. Loktev, Preprint ITF-87-127R, Kiev (1987); Yu. B. Gaididei and V. M. Loktev, Phys. Status Solidi B **147**, 307 (1988).
[9] S. G. Ovchinnikov, Zh. Éksp. Teor. Fiz. **102**, 127 (1992) [Sov. Phys. JETP **75**, 67 (1992)].
[10] A. Svane, Phys. Rev. Lett. **68**, 1900 (1992).
[11] E. L. Nagaev, *Physics of Magnetic Semiconductors*, Mir, Moscow (1983).
[12] T. Takahashi, F. Maeda, H. Katayama-Yoshida *et al.*, Phys. Rev. B **37**, 9788 (1988).
[13] S. G. Ovchinnikov and I. S. Sandalov, Physica C (Amsterdam) **161**, 607 (1989).
[14] S. G. Ovchinnikov and O. G. Petrakovskiĭ, Sverkhprovodimost: Fiz., Khim., Tekh. **3**, 2492 (1990) [Supercond., Phys. Chem. Technol. **3**, 1709 (1990)].
[15] S. G. Ovchinnikov, Zh. Éksp. Teor. Fiz. **104**, 3719 (1993) [JETP **77**, 781 (1993)].
[16] S. V. Lovtsov and V. Yu. Yushankhai, Physica C (Amsterdam) **179**, 159 (1991).
[17] R. O. Zaĭtsev, Zh. Éksp. Teor. Fiz. **68**, 207 (1975) [Sov. Phys. JETP **41**, 100 (1975)].
[18] Yu. A. Izyumov, N. M. Plakida, and Yu. N. Skryabin, Usp. Fiz. Nauk **159**, 621 (1989) [Sov. Phys. Usp. **32**, 1060 (1989)].
[19] V. V. Val'kov and S. G. Ovchinnikov, Teor. Mat. Fiz. **50**, 466 (1982) [Theor. Math. Phys. **50**, 306 (1982)].
[20] P. Horsch and W. von der Linden, Z. Phys. B **72**, 181 (1988).
[21] W. Nolting, L. Haunert, and G. Borstel, Phys. Rev. B **46**, 4426 (1992).
[22] V. A. Gavrichkov, M. Sh. Erukhimov, S. G. Ovchinnikov, and I. S. Édel'man, Zh. Éksp. Teor. Fiz. **90**, 1275 (1986) [Sov. Phys. JETP **63**, 744 (1986)].
[23] W. Nolting, W. Borgiel, and G. Borstel, Phys. Rev. B **37**, 7663 (1988).
[24] F. C. Zang and T. M. Rice, Phys. Rev. B **37**, 3759 (1988).
[25] V. J. Emery and G. Reiter, Phys. Rev. B **38**, 4547 (1988).
[26] L. M. Roth, Phys. Rev. Lett. **60**, 379 (1988).
[27] A. F. Barabanov, R. O. Kuzyan, L. A. Maksimov, and G. V. Uĭmin, Sverkhprovodimost: Fiz., Khim., Tekh. **3**, 8 (1990) [Supercond., Phys. Chem. Technol. **3**, 8 (1990)].
[28] S. G. Ovchinnikov, J. Phys. C **20**, 933 (1987).
[29] G. Martínez and P. Horsch, Phys. Rev. B **44**, 317 (1991).
[30] E. Dagotto, F. Ortolani, and D. Scalapino, Phys. Rev. B **46**, 3183 (1992).
[31] Y. Ohta, K. Tsutsui, W. Koshibae *et al.*, Phys. Rev. B **46**, 14022 (1992).
[32] A. F. Barabanov, L. A. Maksimov, and G. V. Uĭmin, JETP Lett. **47**, 622 (1988).
[33] D. M. Frenkel, R. J. Gooding, B. I. Shraiman, and E. D. Siggia, Phys. Rev. B **41**, 350 (1990).
[34] H. J. Schmidt and Y. Kuramoto, Physica B (Amsterdam) **163**, 443 (1990).
[35] R. Eder and K. W. Becker, Z. Phys. B **79**, 333 (1990).
[36] A. F. Barabanov, L. A. Maksimov, and L. E. Zhukov, Phys. Lett. A **181**, 325 (1993).
[37] J. Ashkenazi and C. G. Kuper, Physica C (Amsterdam) **162–164**, 767 (1989).
[38] V. F. Elesin, V. A. Kashurnikov, L. A. Openov, and A. I. Podlivaev, Zh. Éksp. Teor. Fiz. **99**, 237 (1991) [Sov. Phys. JETP **72**, 133 (1991)].
[39] I. S. Sandalov and M. Richter, Phys. Rev. B **50**, 12855 (1994).
[40] Pu Fu-Cho, Dokl. Akad. Nauk SSSR **131**, 546 (1960) [Sov. Phys. Dokl. **5**, 321 (1960)].

Translated by P. Shelnitz